

University of Alabama in Huntsville

LOUIS

Honors Capstone Projects and Theses

Honors College

10-17-2023

Development of an Innovative Transonic Linear Cascade for Aerodynamic Loss Assessments

Andy Thien Hoang

Follow this and additional works at: <https://louis.uah.edu/honors-capstones>

Recommended Citation

Hoang, Andy Thien, "Development of an Innovative Transonic Linear Cascade for Aerodynamic Loss Assessments" (2023). *Honors Capstone Projects and Theses*. 855.
<https://louis.uah.edu/honors-capstones/855>

This Thesis is brought to you for free and open access by the Honors College at LOUIS. It has been accepted for inclusion in Honors Capstone Projects and Theses by an authorized administrator of LOUIS.



Honors College

Frank Franz Hall

+1 (256) 824-6450 (voice)

+1 (256) 824-7339 (fax)

honors@uah.edu

Honors Thesis Copyright Permission

This form must be signed by the student and submitted with the final manuscript.

In presenting this thesis in partial fulfillment of the requirements for Honors Diploma or Certificate from The University of Alabama in Huntsville, I agree that the Library of this University shall make it freely available for inspection. I further agree that permission for extensive copying for scholarly purposes may be granted by my advisor or, in his/her absence, by the Chair of the Department, Director of the Program, or the Dean of the Honors College. It is also understood that due recognition shall be given to me and to The University of Alabama in Huntsville in any scholarly use which may be made of any material in this thesis.

Andy Hoang

Student Name (printed)

Andy

Student Signature

10/17/2023

Date

Contents

Abstract.....	4
Acknowledgements.....	5
Nomenclature.....	6
List of Figures.....	7
List of Tables.....	7
CHAPTER 1. Introduction.....	8
CHAPTER 2. Experimental Facility and Apparatus.....	9
2.1 Supersonic / Transonic Wind Tunnel.....	9
2.2 Linear Cascade.....	9
CHAPTER 3. Experimental Apparatus and Procedures.....	11
3.1 Instrumented Blade.....	11
3.2 Pressure Measurements.....	11
3.3 Temperature Measurements.....	12
3.4 One-Dimensional Traverse.....	12
3.5 Downstream Aerodynamic Loss Measurements.....	13
3.6 Data Acquisition and Processing.....	13
CHAPTER 4. Summary and Conclusions.....	15
References.....	16
Figures.....	17

Abstract

The present thesis describes the development of an innovative transonic linear cascade for aerodynamic loss assessments, measurements, and evaluations to account for the effects of turbine blade surface texture and surface finish. A currently employed transonic linear cascade is to be modified and enhanced for this purpose. The previous linear cascade is in place and fully operational within the UAH Supersonic Wind Tunnel (or SS/TS/WT – supersonic/transonic/wind tunnel) located within the Propulsion Research Center (PRC) of the University of Alabama in Huntsville (UAH). The alterations required to this facility to allow probe access and traversing capability for measurement and evaluation of elaborate spatially-resolved aerodynamic loss experimental data are significant. In addition to many components which are in place, also required are new experimental equipment and apparatus, experimental procedures, and analysis tools. The components, apparatus, modifications, and enhancements which are underway to provide these capabilities are described within the present thesis. Within the linear cascade, the inlet Mach number is approximately 0.29, and the cascade outlet Mach number between blade wakes is approximately 0.87. The blade tip to be considered is flat and smooth without a squealer tip or squealer recess. Three types of probes are employed to provide turbine blade wake survey information at location which is 0.25 axial chord lengths downstream of the trailing edges of the turbine blades: (a) miniature Kiel probe for measurement of local stagnation pressure, (b) total-static probe for simultaneous measurement of local stagnation pressure and local static pressure, and (c) thermocouple probe for measurement of local recovery temperature. Also, to be measured are turbine blade surface static pressure distributions. The presently proposed aerodynamic loss data are especially useful, because they are obtained to include the effects of compressibility, within a cascade configuration which matches an operating engine arrangement, at appropriate Mach number and Reynolds number values.

Acknowledgements

Mr. Preston McMahan is acknowledged for his assistance with developing the three-dimensional models of Figures 1-6. Mr. Chase Herrin is acknowledged for his work in creating Figures 23 and 24. NASA Marshall Space Flight Center (Contract Number 8ONSSC23PCO41) is acknowledged for sponsoring the present study.

Nomenclature

C_x	=	axial chord length
M	=	Mach number
PS	=	Pressure Side
P_s	=	static pressure
P_o	=	stagnation pressure
SS	=	Suction Side
x	=	dimensional axial coordinate
x/C_x	=	dimensional axial coordinate for normalization

List of Figures

- Figure 1. Three-dimensional isometric view of the traverse mounted above the linear cascade at the inlet.
- Figure 2. Three-dimensional isometric view of the traverse mounted above the linear cascade at the exit.
- Figure 3. Three-dimensional isometric view of the traverse mounted above the linear cascade.
- Figure 4. Front view at the inlet of the flow passage of the linear cascade.
- Figure 5. View at the exit of the flow passage of the linear cascade.
- Figure 6. Enlarged view of the pitot static probes, probe guides, thermocouples, and neoprene strips.
- Figure 7. Schematic diagram of the linear cascade. Dimensions given in mm.
- Figure 8. Schematic diagram of the casing wall of the linear cascade. Dimensions given in mm.
- Figure 9. Top view of the end wall assembly of the linear cascade without the casing wall.
- Figure 10. Top view of the casing wall assembly of the linear cascade.
- Figure 11. Three-dimensional isometric view of the linear cascade assembly at the inlet.
- Figure 12. Three-dimensional isometric view of the linear cascade assembly at the exit.
- Figure 13. Three-dimensional isometric view of the linear cascade assembly.
- Figure 14. Central turbine blade pressure tap locations numerically labeled.
- Figure 15. Central turbine blade pressure tap dimensional x locations. Dimensions given in millimeters.
- Figure 16. Central turbine blade pressure tap x/C_x locations.
- Figure 17. Bottom view of the central turbine blade showing the cooling passage holes with pressure tap connection locations.
- Figure 18. Three-dimensional isometric view of the PCB-6-KL pitot static probe.
- Figure 19. Three-dimensional isometric view of the KCC-8 Kiel probe.
- Figure 20. Three-dimensional isometric view of Omega 5TC-GG-T-24-72 Type T thermocouple.
- Figure 21. Three-dimensional isometric view of the one-dimensional traverse.
- Figure 22. Three-dimensional isometric view of the one-dimensional traverse.
- Figure 23. Aerodynamic loss measurement's locations and arrangements.
- Figure 24. Enlarged view of the aerodynamic loss measurement's locations and arrangements.
- Figure 25. Schematic diagram of the data acquisition system.

List of Tables

- Table 1. Central blade pressure tap Locations.

CHAPTER 1. Introduction

Surface roughness on aerodynamic airfoils and turbine blades exerts a substantial influence on the overall energy dissipation and second law losses caused by skin friction, often resulting in heightened thermal stress levels within adjacent solid materials. Additional information regarding the effects of surface roughness on turbine blades is provided in Hohenstein et al. (2013) and Mulleners et al. (2014). Within the present study, an existing transonic linear cascade (operating as part of the UAH Supersonic Wind Tunnel or SS/TS/WT –supersonic/transonic/wind tunnel located within the Propulsion Research Center of the University of Alabama in Huntsville) is modified and enhanced to allow innovative investigation of the impact of surface roughness and texture on the downstream aerodynamic losses from a turbine blade. In particular, to implement this new investigation, new designs for the casing wall, traverse, and cascade traverse assembly are required. Also needed are new experimental equipment and apparatus, experimental procedures, and analysis tools. The components, apparatus, modifications, and enhancements which are underway to provide these capabilities are described within the present thesis.

During operation, in regard to linear cascade flow characteristics, the inlet Mach number is approximately 0.29, and the cascade exit Mach number between blade wakes is approximately 0.87. The linear cascade assembly consists of a 5-blade configuration which models an operating engine arrangement. The central blade of this configuration has the capability to contain a textured surface roughness finish. Pressure measurements are to be recorded within the central blade's wake which is 0.25 axial chord lengths downstream of the trailing edges of the blade. Since the pressure surveys are conducted at 50 percent span of the central blade, tip gap effects are not considered. As a result, the central blade tip is flat and smooth without a squealer rim or squealer recess. Three types of probes are to be employed to provide turbine blade wake survey information: (a) miniature Kiel probe for measurement of local stagnation pressure, (b) total-static probe for simultaneous measurement of local stagnation pressure and local static pressure, and (c) thermocouple probe for measurement of local recovery temperature. Also, to be measured are turbine blade surface static pressure distributions.

The presently proposed aerodynamic loss data are especially useful, because they are obtained to include the effects of compressibility, within a cascade configuration which matches an operating engine arrangement, at appropriate Mach number and Reynolds number values.

CHAPTER 2. Experimental Facility and Apparatus

Described within the present chapter are the Supersonic / Transonic Wind Tunnel, and the linear cascade.

2.1 Supersonic / Transonic Wind Tunnel

The SS/TS/WT (supersonic/transonic/wind tunnel) experimental facility employed for the present investigation is a blow-down facility, located within the UAH Propulsion Research Center, and is described by Collopy et al. (2022). High-speed flows are provided using an elaborate air pressure tank supply system with specially provisioned flow and pressure control regulating valves. The wind tunnel tanks air supply has a total volume of 50 m³. The facility includes three parallel wind tunnel legs each with a different test section. Only one of the three parallel legs is employed for the present study. For the present investigation, a subsonic nozzle directs the mainstream inlet flow through a turbulence bar grid. This grid is located upstream of the test section entrance to produce a cascade inlet turbulence intensity magnitude of 6 to 7 percent. This linear cascade, contained within the test section, is employed to investigate the aerodynamic losses due to varied surface roughness of a transonic turbine blade.

2.2 Linear Cascade

The linear cascade assembly used for the present study includes a newly designed casing wall, a one-dimensional traverse, several different pressure probes each with a thermocouple attached, pitot probe guides, and neoprene strip sealing pads. The new casing wall is designed with one slot to allow for two pressure probes to be inserted at the same time through the casing wall. These items are to be used for simultaneous measurements of local stagnation pressure, local static pressure, and local recovery temperature during experimentation. A one-dimensional traverse is mounted above the casing wall and contains items with which to mount and orient the different probes which are employed for the investigation. These probes are inserted into the cascade exit flow through a slot which is lined with neoprene strips to prevent any air leakage through the casing wall. Note that each pressure probe contains a probe guide attached that allows the probe to traverse between the two neoprene strips.

Figures 1-3 show full concept assembly drawings of the linear cascade, including the probes, traverse, and neoprene strips. Figures 4 and 5 present views from the inlet and exit of the flow to illustrate the pressure probe tip positions at 50 percent span of the central blade. Figure 6 shows an enlarged view of the pitot static probes, thermocouples, probe guides, and neoprene stripping, including a portion of the casing wall.

A schematic diagram of the currently employed linear cascade, with dimensions given in millimeters, is shown in Figure 7. The cascade includes four flow passages with five complete blades. Shown are the locations of the textured central turbine blade, pitchwise bleed slots, and tailboard. Spanwise bleed slots are also included at the cascade section inlet. The central blade is textured, and a one-

dimensional traverse is mounted above the casing wall to allow for measurements along the wake of the central turbine blade. At the inlet of the cascade, a Kiel probe is installed to allow measurement of local stagnation pressure, note that this probe is removed as downstream aerodynamic loss data are measured. Thermocouples are secured to each pressure probe to determine inlet recovery temperature. The same tip gap value is employed for all three central blades within the cascade. As previously mentioned, the central blade tip is flat and smooth without a squealer rim or recess.

Within the cascade, the axial blade chord length is 74.73 mm. The flow inlet angle, exit angle, and total turning angle are 27.2° , 61.3° and 88.5° , respectively. The true blade chord and the pitch measure 92.67 mm, and 75.93 mm, respectively. The total pitch wise distance between the exterior blades is 303.71 mm. At the inlet of the cascade, the distance between the sidewalls is 270.13 mm. The experimental blade span is 85 mm. The true blade span is 119.3 mm. A single adjustable tailboard is located downstream of the blade rows. The dimensions of the cascade and turbine blades are scaled based on engine geometry. Within the present linear cascade, no relative motion is present between the blade and the casing.

The estimated value of boundary layer thickness, relative to the casing surface, near the leading edge of each blade, is 4.0 mm or about 5.5 percent of the axial chord length C_x . The associated von Karman shape factor is estimated to be 1.31 to 1.34. At the cascade inlet, flow static temperature, static pressure, stagnation pressure, sonic velocity, flow velocity, and Mach number are approximately 321.2 K, 192.1 kPa, 204.3 kPa, 359.3 m/sec, 105.6 m/sec, and 0.294, respectively. Near the cascade exit between blade wakes, static pressure, and Mach number are approximately 101.4 kPa and 0.87, respectively. The resulting Reynolds number, based upon C_x and inlet flow conditions, is 815,890. The associated inlet temperature and inlet isentropic Mach number are measured at the inlet of the cascade which is upstream of the blade row. The velocity boundary layer and temperature boundary layer are fully turbulent at this same location.

Additional discussion of the cascade apparatus and flow conditions is provided by Collopy et al. (2022).

A schematic diagram of the newly designed casing wall for the linear cascade, with dimensions given in millimeters, is shown in Figure 8. Shown in the figure is a single slot measuring 14 mm in width and 152.4 mm in length that is cut through the casing wall a quarter chord ($0.25C_x$) length from the trailing edge of the central blade. The purpose of the slot is to allow the pressure probes, attached to the one-dimensional traverse, to traverse continuously at various points during testing for pressure surveys. The casing wall is constructed using 19.05 mm thick acrylic. Figures 9 and 10 show top views of the end wall linear cascade assembly with and without the casing wall attached. Figures 11, 12, and 13 show three-dimensional views of the linear cascade assembly with the new casing wall.

CHAPTER 3. Experimental Apparatus and Procedures

Described within the present chapter are apparatus and procedures related to pressure measurements, temperature measurements, and the one-dimensional traverse. Also included in the present chapter are topics regarding the instrumented blade, downstream aerodynamic loss assessment locations, and data acquisition system.

3.1 Instrumented Blade

Each central turbine blade to be employed has a total of 22 pressure taps to obtain surface static pressure measurements. Figure 14 shows a top view of the central turbine blade with pressure tap locations numbered along the pressure side and suction side of the blade. The axial chord length of the central turbine blade is 74.79 millimeters. Figure 15 shows the pressure tap axial locations with dimensions given in millimeters. Figure 16 presents the same pressure tap locations normalized with the axial chord length (x/C_x). Table 1 displays the tabulated measurements of the pressure tap locations based on dimensional axial location, and normalized axial location. Figure 17 shows a view of the bottom of the central turbine blade showing pressure tap connection locations.

3.2 Pressure Measurements

Along the wake of the blade, simultaneous pressure measurements of local stagnation pressure and local static pressure will be conducted using a PCB-6-KL pitot static probe from United Sensor Corporation. Figure 18 shows a three-dimensional isometric view of the PCB-6-KL pitot static probe. At the inlet of the cascade, as well as at the cascade exit at the same locations as the pitot static probe, stagnation pressure is measured using a United Sensor Corporation KCC-8 Kiel probe. Figure 19 shows a three-dimensional isometric view of the KCC-8 Kiel probe. Each of these pressures is measured using a Honeywell FPA 060 C54985172080 digital pressure transducer, or a Honeywell model FP2000 digital pressure transducer. Each transducer is connected to a National Instruments card, NI 9209, and a NI 9923 terminal block, mounted within a NI CompactDAQ USB Chassis, NI cDAQ-9174. These devices together convert the analog voltage signal from the transducers into a digital signal, which is acquired using LabVIEW Full Development System 2020 version 20.0.1 software. Note that this same pressure measurement system is also employed for measurements of static pressure along the surfaces of the different instrumented turbine blades.

The absolute pressure transducers are calibrated in a multiple fashion, using a compressed air deadweight tester. The pressure transducers send signal voltages through the NI 9923 terminal block to a NI 9209 data acquisition card mounted within a National Instruments NI cDAQ-9174 chassis. Digital signals are acquired using LabVIEW Full Development System 2020 version 20.0.1 software for pressure increments of 34.5 kPa (5 psi) ranging from ambient to 241.3 kPa (35 psi) above ambient. The voltage signal for each pressure transducer is recorded using Microsoft Office EXCEL version 2013 software, along with the corresponding reference pressure measurement. Resulting signal voltages and corresponding

absolute pressure values are used to determine calibration equation relationships for each pressure transducer.

For more details on these measurement systems, including pressure transducer calibration procedures, see Collopy et al. (2022).

3.3 Temperature Measurements

Temperatures of the air stream at the wake of the central turbine blade are measured using two calibrated Omega 5TC-GG-T-24-72 Type T thermocouples. Figure 20 shows a three-dimensional isometric view of the Omega 5TC-GG-T-24-72 Type T thermocouple. Thermocouple signals are acquired using a National Instruments NI 9213 thermocouple input card mounted within a National Instruments NI cDAQ-9174 chassis. These devices together convert the analog voltage signal from the transducers into a digital signal which is acquired using LabVIEW Full Development System 2020 version 20.0.1 software. The resulting data from this program is processing using a Dell Precision T1700 with an Intel Core i7 - 4790 CPU Processor computer workstation.

Thermocouples are calibrated using an Omega Thermoregulator HCTB-3030 Constant Temperature Liquid Circulating bath. Reference temperatures are measured with a Fluke Hart Scientific Division 1523 thermometer. Voltage signals are acquired with the thermocouple input card, and the previously described LabVIEW Full Development System 2020 version 20.0.1 software and recorded using Microsoft Office EXCEL version 2013 software. These measured values are used to determine a calibration conversion equation for each thermocouple junction.

Collopy et al. (2022) provide additional details on thermocouple measurement apparatus and procedures, and in regard to thermocouple calibration.

3.4 One-Dimensional Traverse

To collect multiple data points along the wake during operation, a one-dimensional traverse system is employed. Figures 21 and 22 show three-dimensional views of the one-dimensional traverse system. The system provides traversing capabilities in only one direction. This system consists of a NEMA-17 with T5 pulley stepper motor, one 12 mm diameter central ultra-precision lead screw, two 12 mm diameter guide rods, a horizontal traverse base, and supports. The NEMA-17 stepper motor is connected to Actobotics X-rails using stepper motor mounts from Adafruit. A 5 mm to 8 mm flexible clamping shaft coupler is used to connect the stepper motor to the central ultra precision lead screw. Flexible clamping shaft couplers transfer rotational motion between two shafts in order to avoid misalignment. A thrust bearing is fixed between the clamping shaft collar and a thru-hole pillow block that mitigates any axial loading on the lead screw. Two 8 mm lead screw nuts with the 19.558 mm pattern are used for the ultra-precision lead screw for the horizontal base. Two 8 mm stainless steel precision shaftings are used as guide rods for the horizontal base. Each guide rod has an 8 mm inner diameter linear ball bearing, or shaft guiding, with 45 mm length. The

linear ball bearings are connected to the horizontal base using 15 mm bore bottom tapped clamping mounts. The single two-phase NEMA-17 with T5 pulley stepper motor (Part number CTP10ELF10MAA00) moves in small, precise, 1.8-degree increments at 200 steps/revolution. The motor is brushless and maintenance-free. The stepper motor is connected to a P70530 Stepper drive device. The stepper drive controls one axis motion with 200-50000 steps/rev resolution, which requires a 5.0 Amp continuous current, and 20-75 VDC input voltage.

3.5 Downstream Aerodynamic Loss Measurements

Static pressure, stagnation pressure, and recovery temperature are to be measured within the wake downstream of the central turbine blade. These probes are attached to the one-dimensional traversing system, such that probe tips are positioned a quarter of an axial chord length ($0.25C_x$) away from the trailing edges of the turbine blades. Figure 23 shows a diagram of the locations and arrangements for the aerodynamic loss measurements. Figure 24 shows an enlarged view of a portion of this diagram. Within Figure 24, probe measurement locations are denoted with tick marks.

3.6 Data Acquisition and Processing

Figure 19 shows a schematic diagram of the data acquisition system which includes the pressure transducers, thermocouples, traverse motor, and the associated NI data acquisition cards. Included within this figure are the P70530 Stepper drives, which are connected to an NI PS-15 Power Supply, which can generate a voltage of 24 VDC and a current of 5 A. The P70530 Stepper drives are connected to a UMI-7772 Universal Motion Interface. The UMI-7772 universal motion interface is connected to a NI PS-15 Power Supply, and to a NI PCI-7342, 2 Axis Stepper Motion Controller. The PCI-7342 offers linear interpolation for coordinating multiple axes, real-time system integration for directly communicating with smooth motion at high velocities. The PCI-7342 is operated using LabVIEW Full Development System 2020 version 20.0.1 commercial motion control software.

Also, connected to the computer with USB cables is a National Instruments cDAQ-9174 chassis. The NI cDAQ-9174 is a four-slot USB chassis, which interfaces with an NI 9209 data acquisition card and an NI 9923 terminal block. In order to operate each Honeywell pressure transducer, each transducer is wired into the NI 9923 terminal block that transmits the differential analog voltage signals from the transducers to a NI 9209 data acquisition card, which is a National Instruments simultaneous bridge module. The NI 9209 data acquisition card is also connected to the National Instruments cDAQ-9174 chassis. The NI 9209 data acquisition card has the capability of sampling four bridge-based sensors up to 50 kHz simultaneously. Within the present study, the NI 9209 data acquisition card is used to acquire bridge output voltages from the Honeywell pressure transducers, as mentioned. Thermocouple signals are acquired using a National Instruments NI 9213 thermocouple input card mounted within a National Instruments NI cDAQ-9174 chassis. The digital signals, which are provided by the NI 9209 data acquisition card, NI 9923 terminal

block, NI 9213 input card, and NI cDAQ-9174 chassis, are acquired and recorded using LabVIEW Full Development System 2020 version 20.0.1 software. The resulting data from this program is processing using a Dell Precision T1700 with an Intel Core i7 - 4790 CPU Processor computer workstation.

CHAPTER 4. Summary and Conclusions

To investigate this impact on aerodynamic losses from turbine blades due to surface roughness and texture, a unique instrumented and innovative transonic linear cascade is under development. Required for this development are a newly designed and manufactured casing wall, a one-dimensional traverse, pitot static probes, Kiel probes, thermocouples, pitot probe guides, neoprene stripping, and a cascade traverse assembly. Operating with transonic conditions with an inlet Mach number of approximately 0.29 and a cascade exit Mach number of around 0.87 between blade wakes, the 5-blade linear configuration models a real-world engine arrangement. The central blade within this configuration is to be installed and tested with surface roughness and texture arrangements. This blade is to be with a flat and smooth central blade tip without a squealer rim or recess. Pressure measurements are to be made within the central blade's wake, positioned $0.25Cx$ axial chord length downstream of the trailing edges of the blades. These measurements are to be made at 50 percent span. To gather turbine blade wake data, three types of probes are to be employed, including a miniature Kiel probe for local stagnation pressure measurement, a total-static probe for simultaneous assessment of local stagnation pressure and local static pressure, and thermocouple probes to measure local recovery temperature. Also, to be measured are turbine blade surface static pressure distributions which account for the effects and influences of turbine blade surface finish.

The presently proposed aerodynamic loss data are especially useful, because they are obtained to include the effects of compressibility, within a cascade configuration which models an operating engine arrangement, at appropriate Mach number and Reynolds number values.

References

- H. Collopy, P.M. Ligrani, H. Xu, M. Fox, Effects of tip gap on transonic turbine blade heat transfer characteristics with pressure side film cooling, *International Journal of Heat and Mass Transfer* 187 (1) (2022) 122513. <https://doi.org/10.1016/j.ijheatmasstransfer.2021.122513>
- Hohenstein, S., Aschenbruck, J., Seume, J. (2013). Aerodynamic effects of non-uniform surface roughness on a turbine blade. *Volume 6A: Turbomachinery*. <https://doi.org/10.1115/gt2013-95433>
- Mulleners, K., Gilge, P., Hohenstein, S. (2014). Impact of surface roughness on the turbulent wake flow of a turbine blade. *Journal of Aerodynamics*, 2014, 1–9. <https://doi.org/10.1155/2014/458757>

Figures

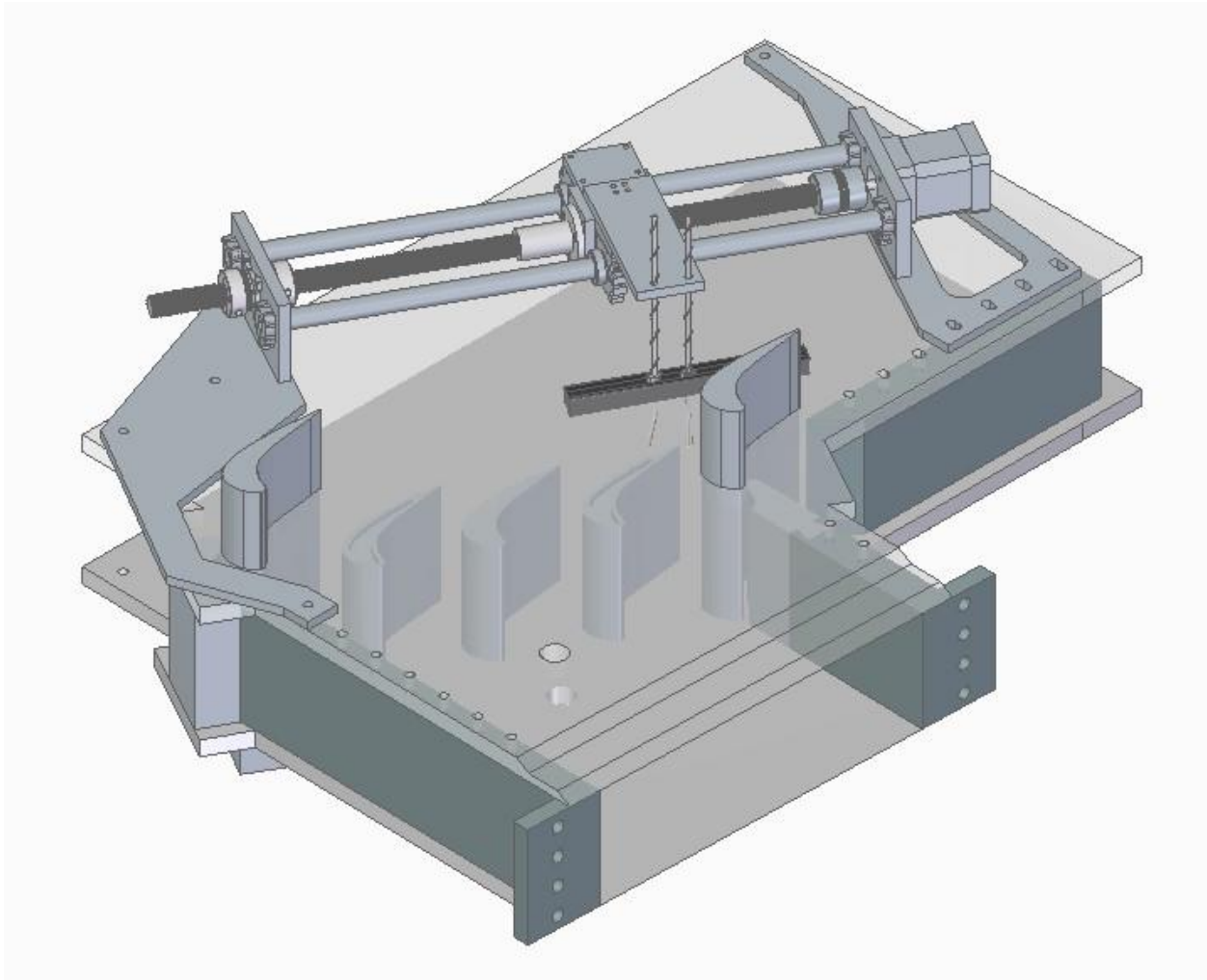


Figure 1. Three-dimensional isometric view of the traverse mounted above the linear cascade at the inlet.

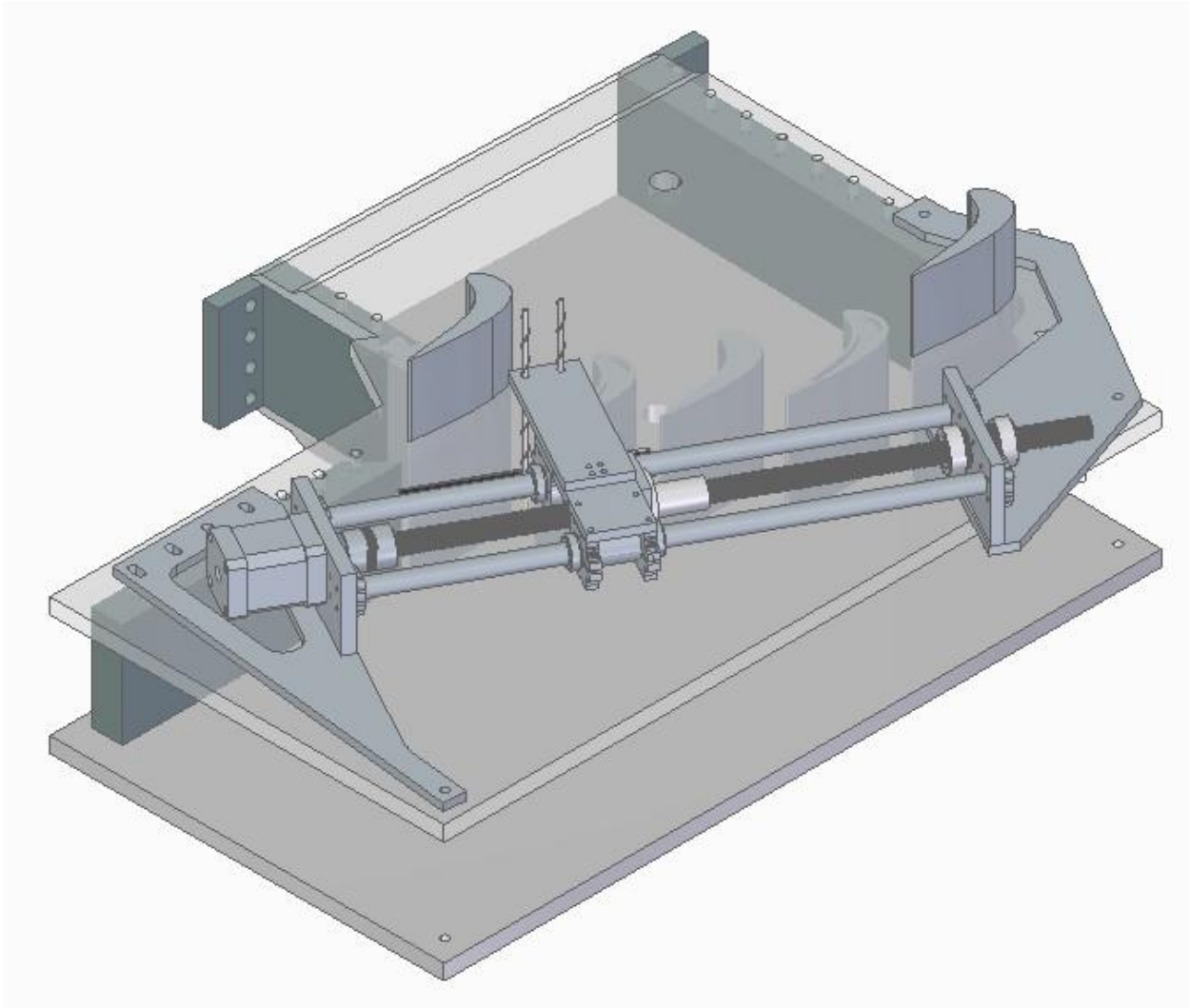


Figure 2. Three-dimensional isometric view of the traverse mounted above the linear cascade at the exit.

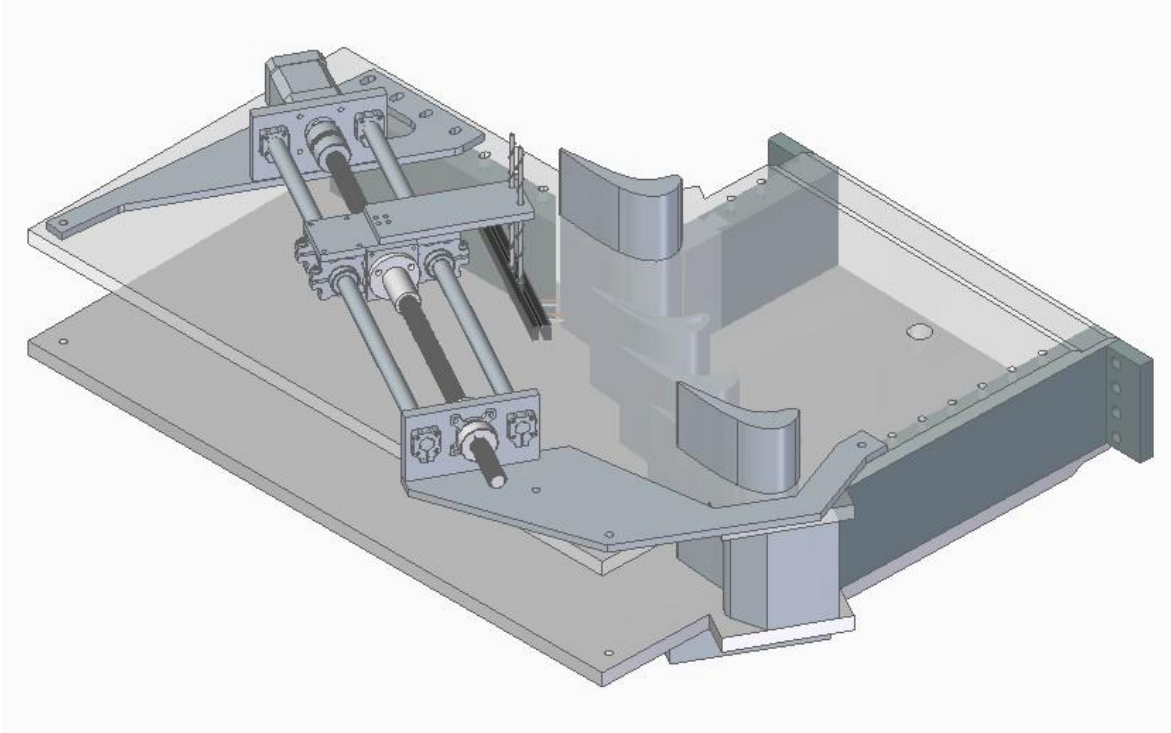


Figure 3. Three-dimensional isometric view of the traverse mounted above the linear cascade.

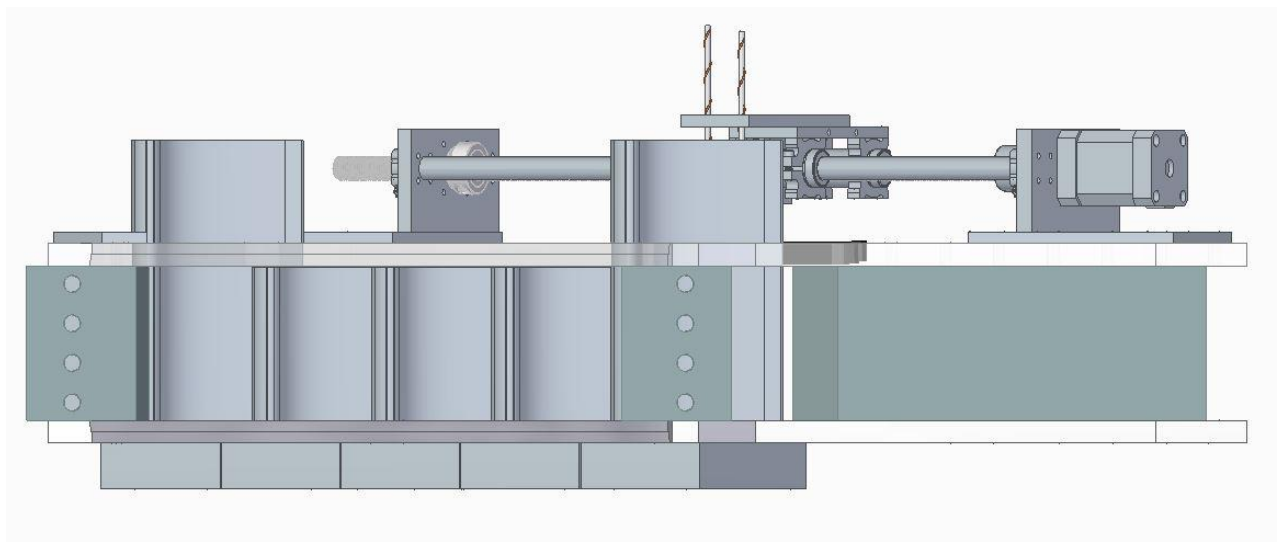


Figure 4. Front view at the inlet of the flow passage of the linear cascade.

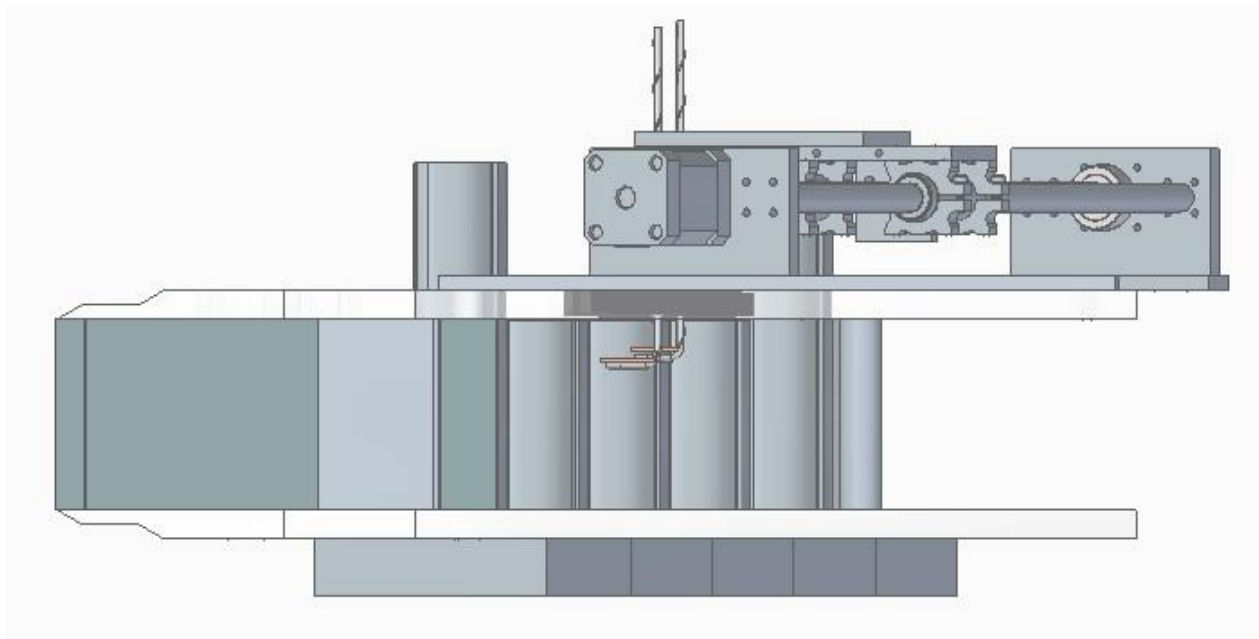


Figure 5. View at the exit of the flow passage of the linear cascade.

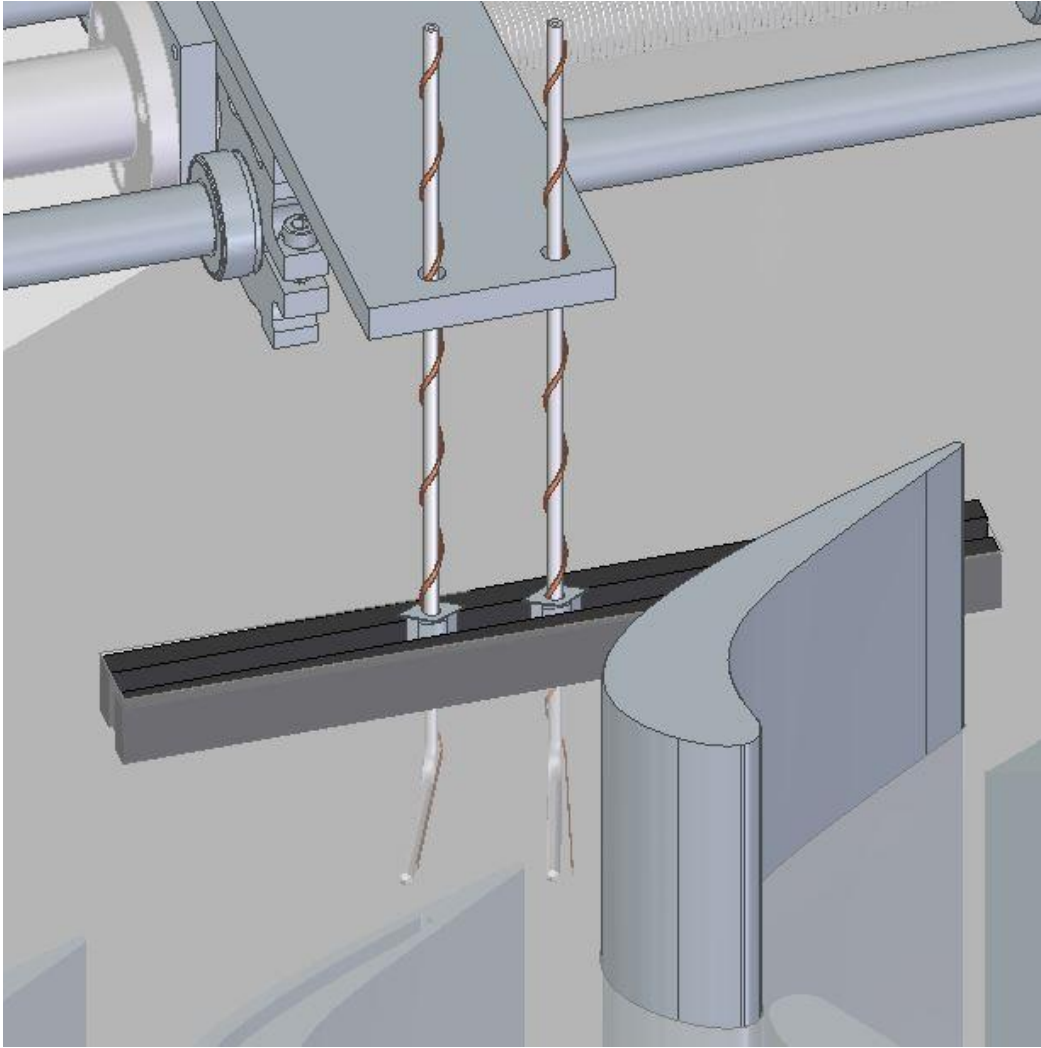


Figure 6. Enlarged view of the pitot static probes, probe guides, thermocouples, and neoprene strips.

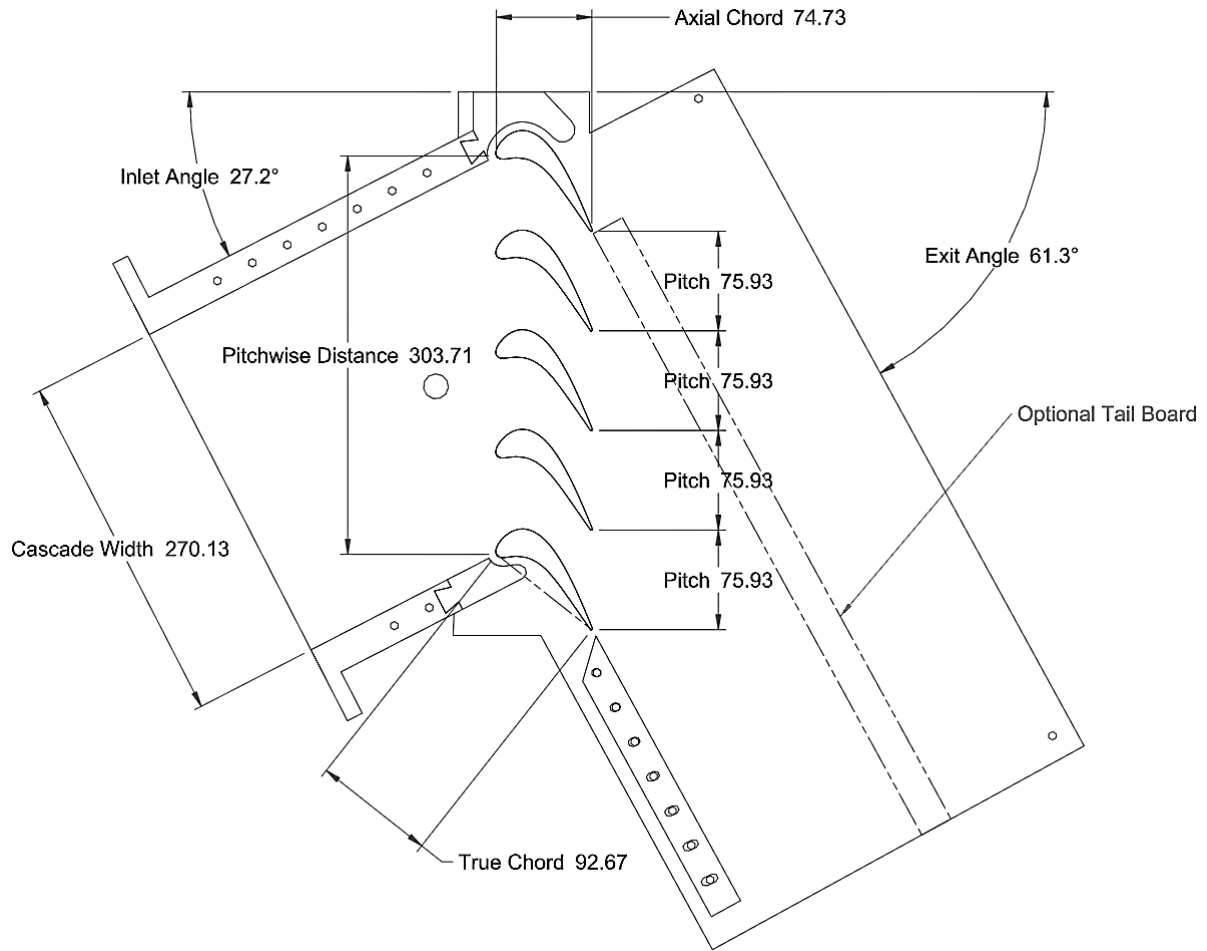


Figure 7. Schematic diagram of the linear cascade. Dimensions given in mm.

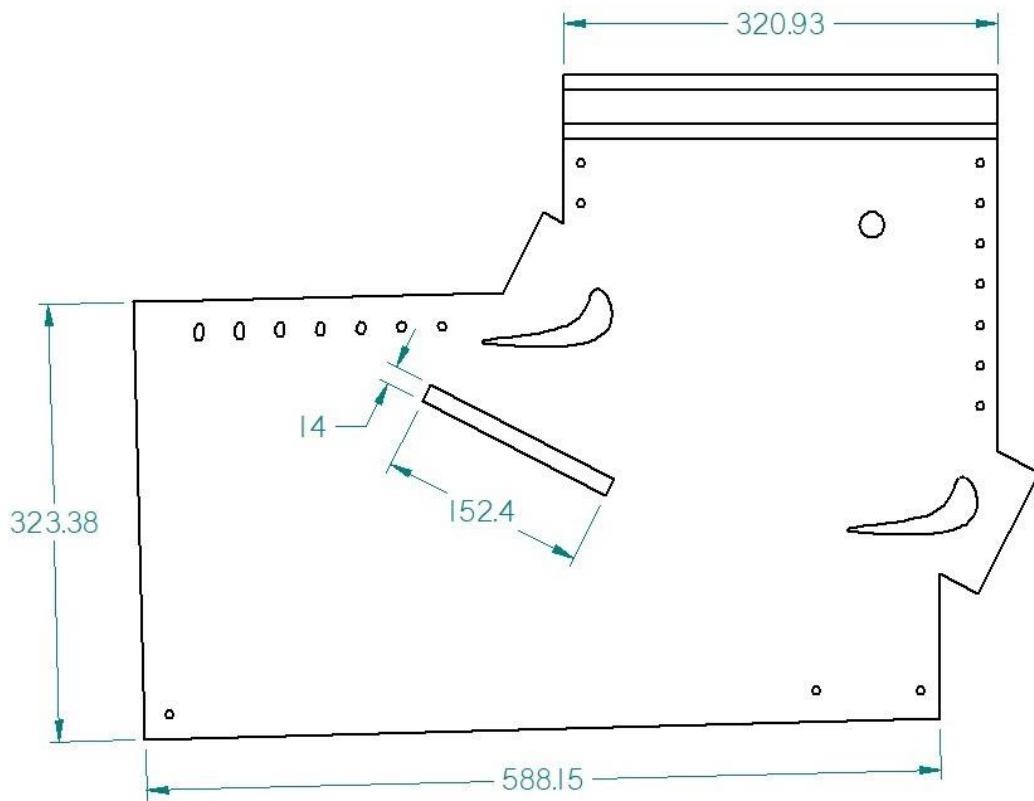


Figure 8. Schematic diagram of the casing wall of the linear cascade. Dimensions given in mm.

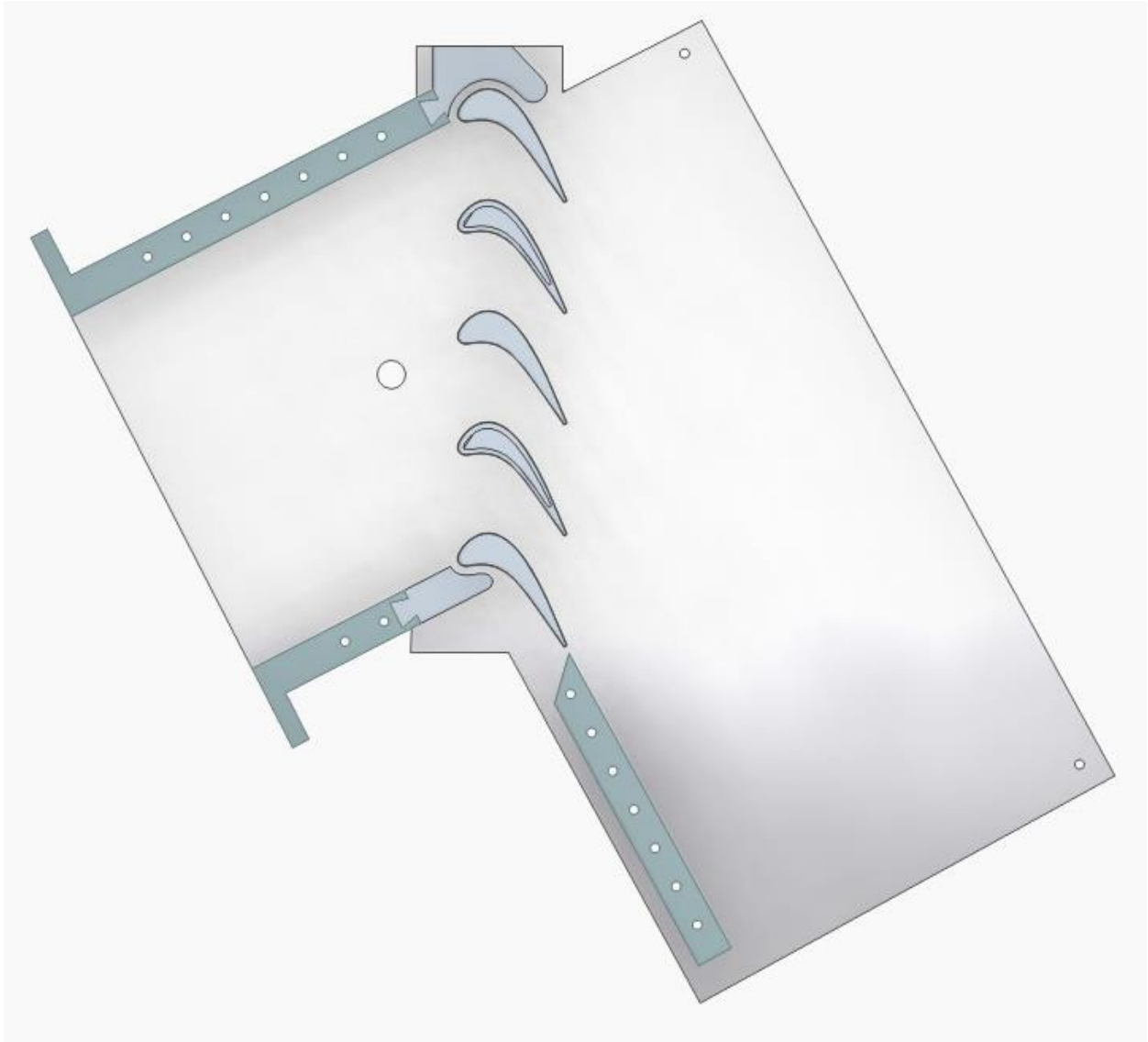


Figure 9. Top view of the end wall assembly of the linear cascade without the casing wall.

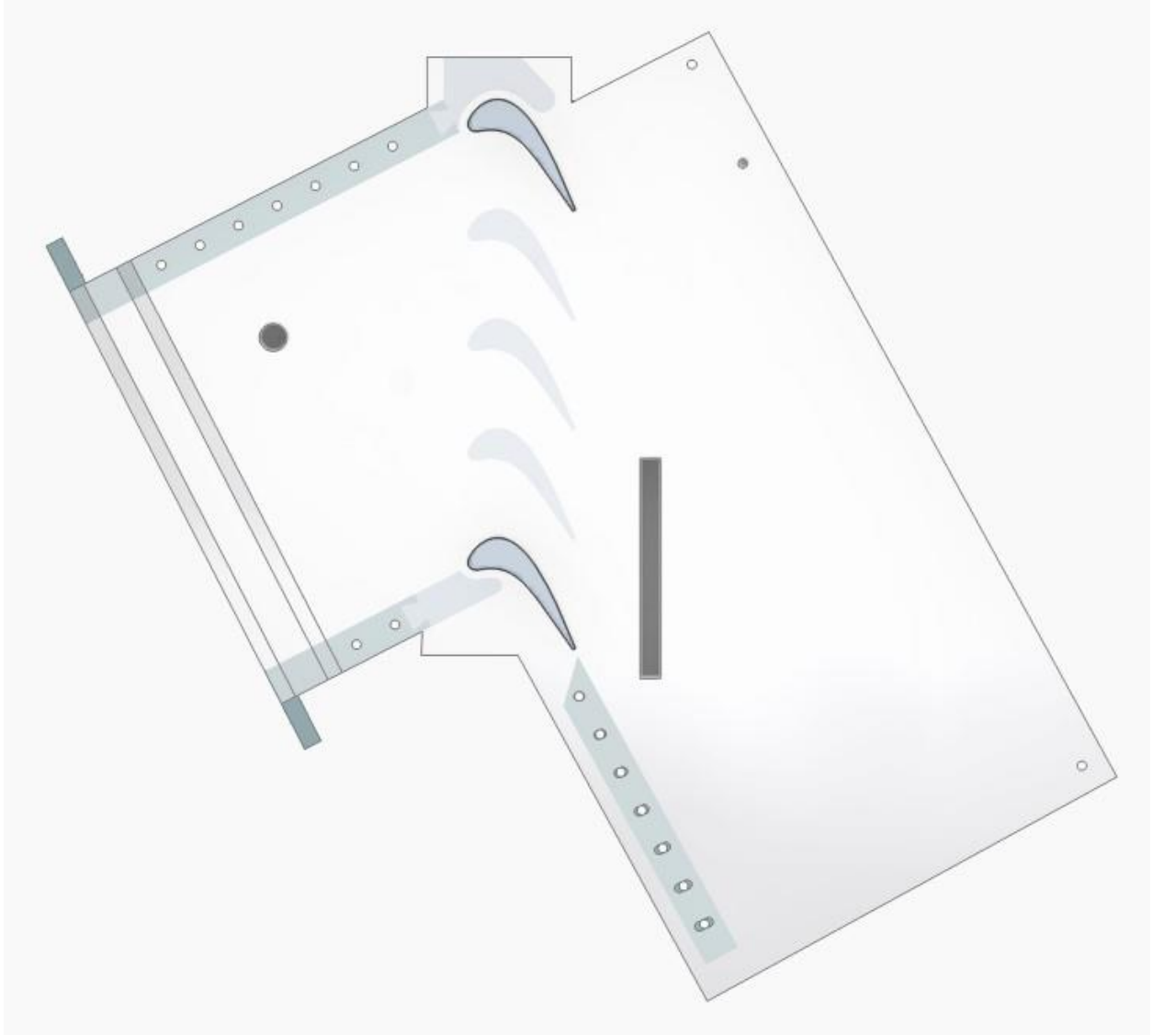


Figure 10. Top view of the casing wall assembly of the linear cascade.

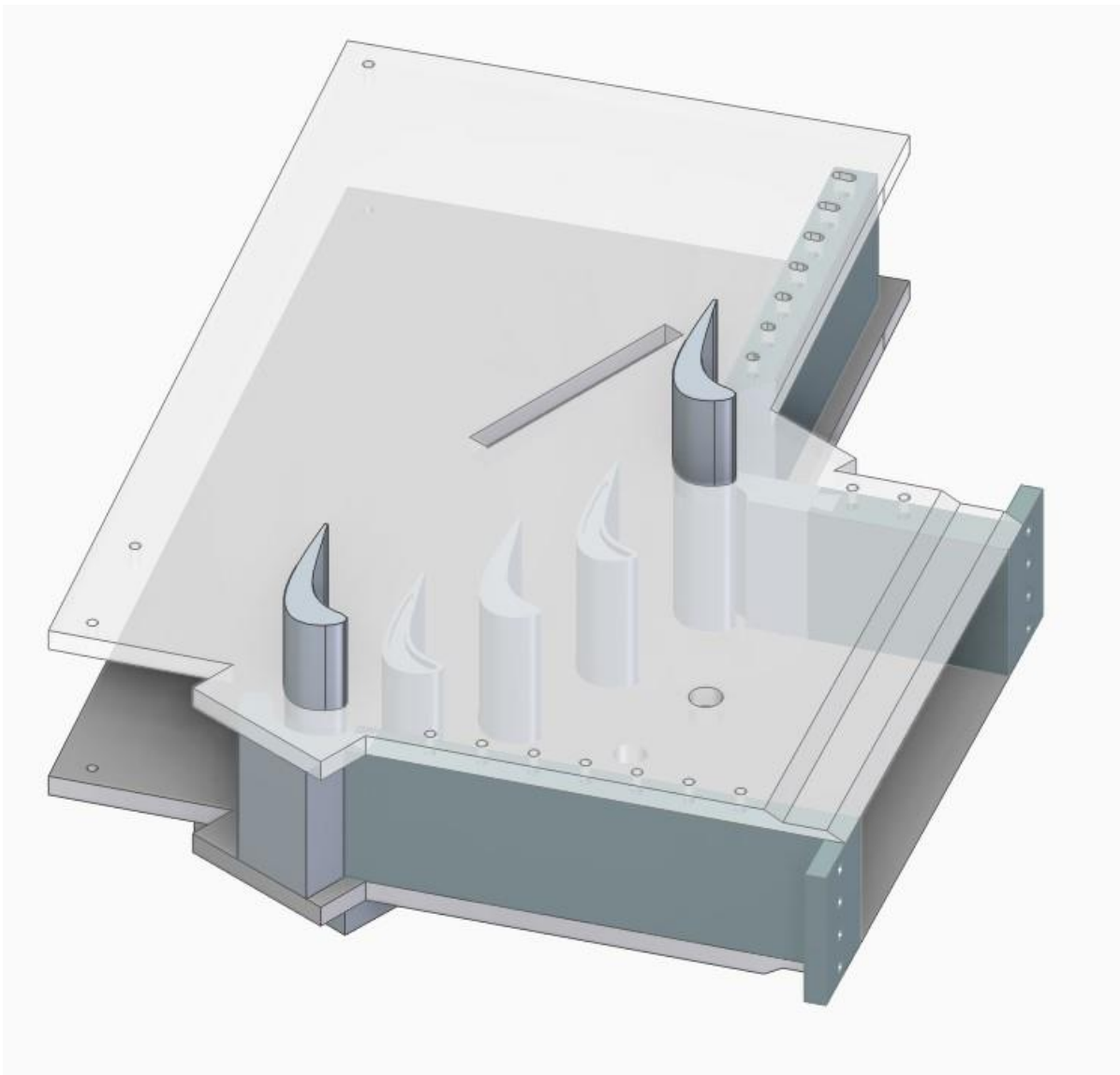


Figure 11. Three-dimensional isometric view of the linear cascade assembly at the inlet.

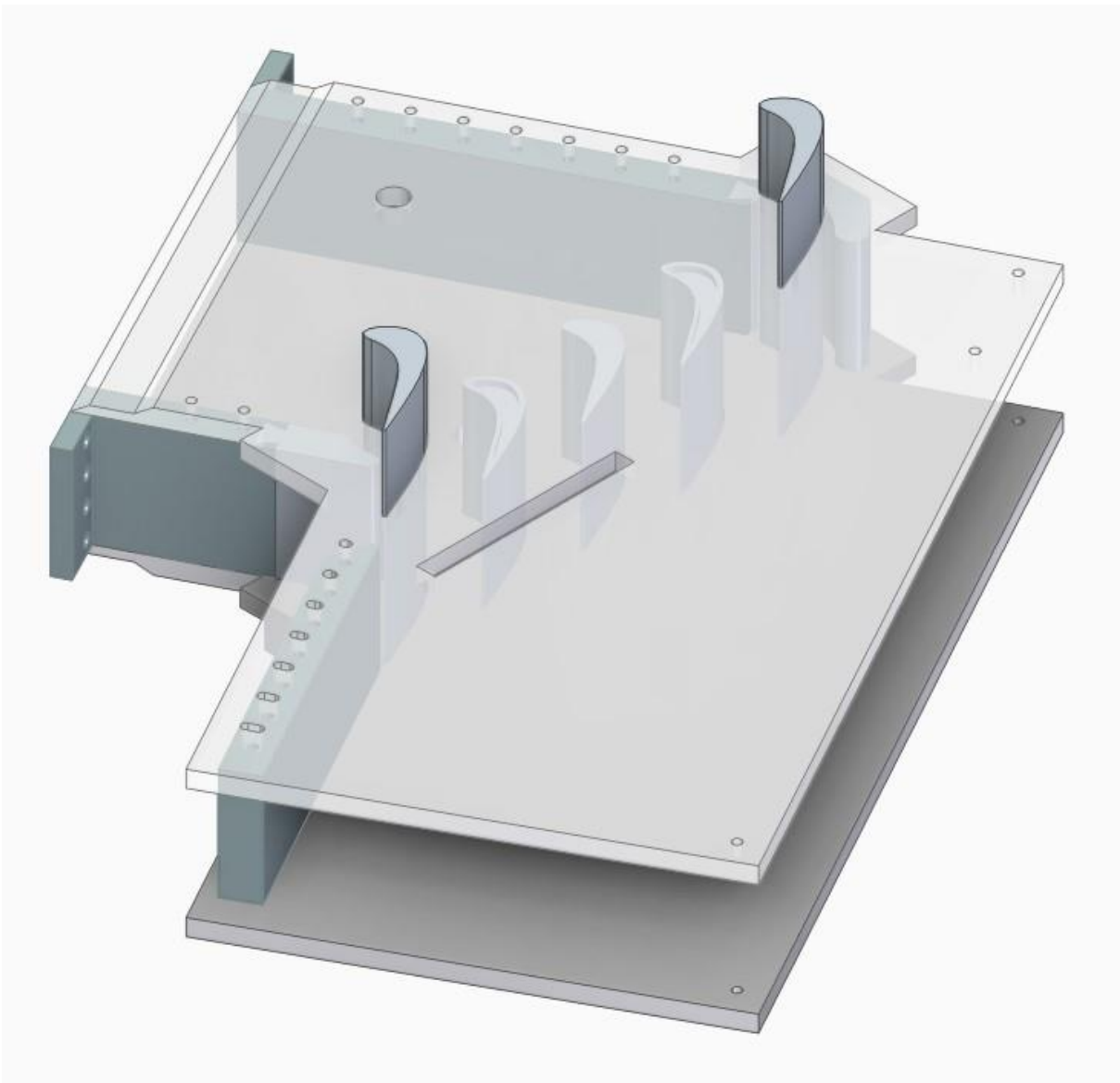


Figure 12. Three-dimensional isometric view of the linear cascade assembly at the exit.

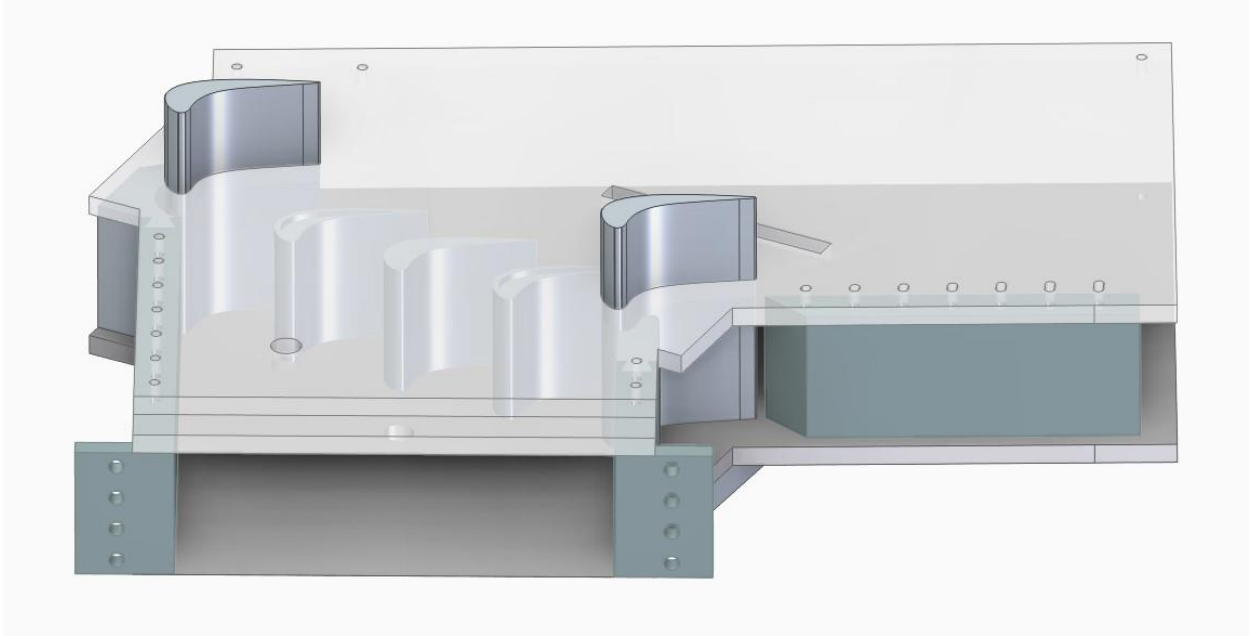


Figure 13. Three-dimensional isometric view of the linear cascade assembly.

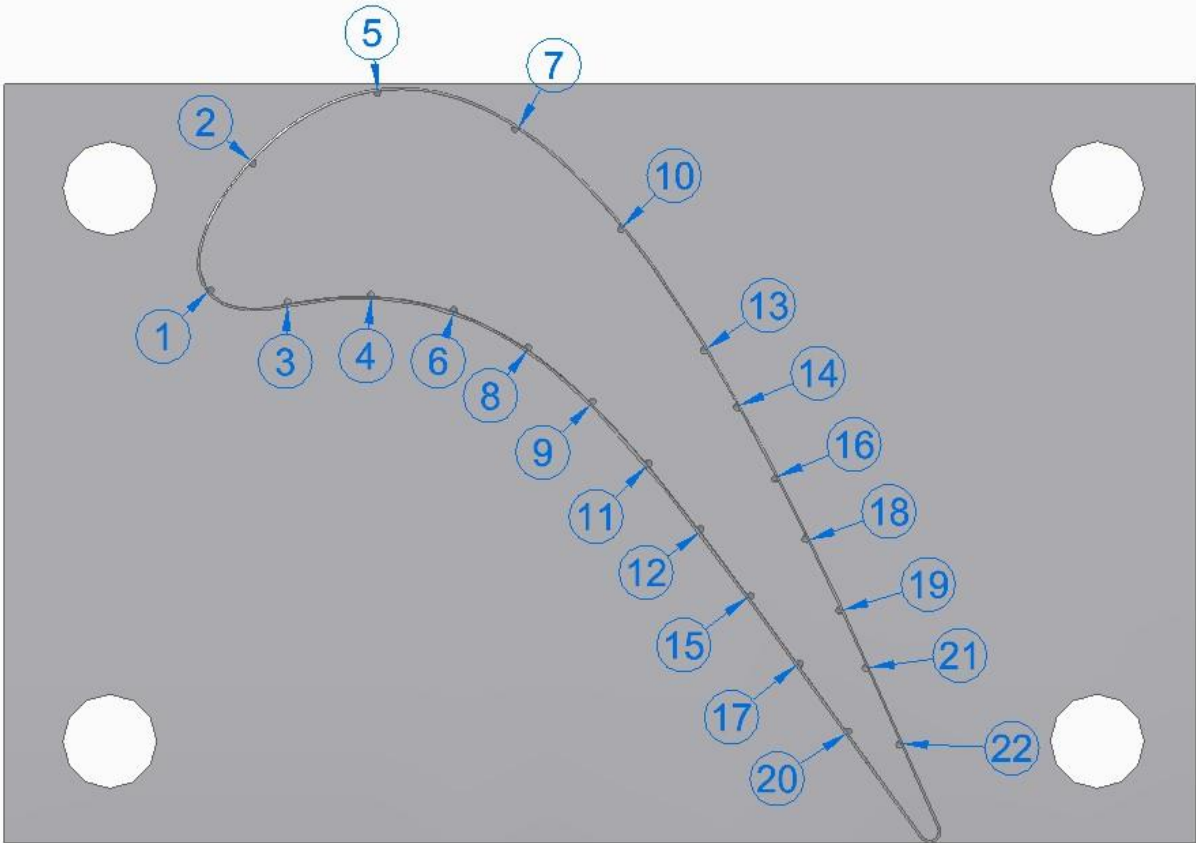


Figure 14. Central turbine blade pressure tap locations numerically labeled.

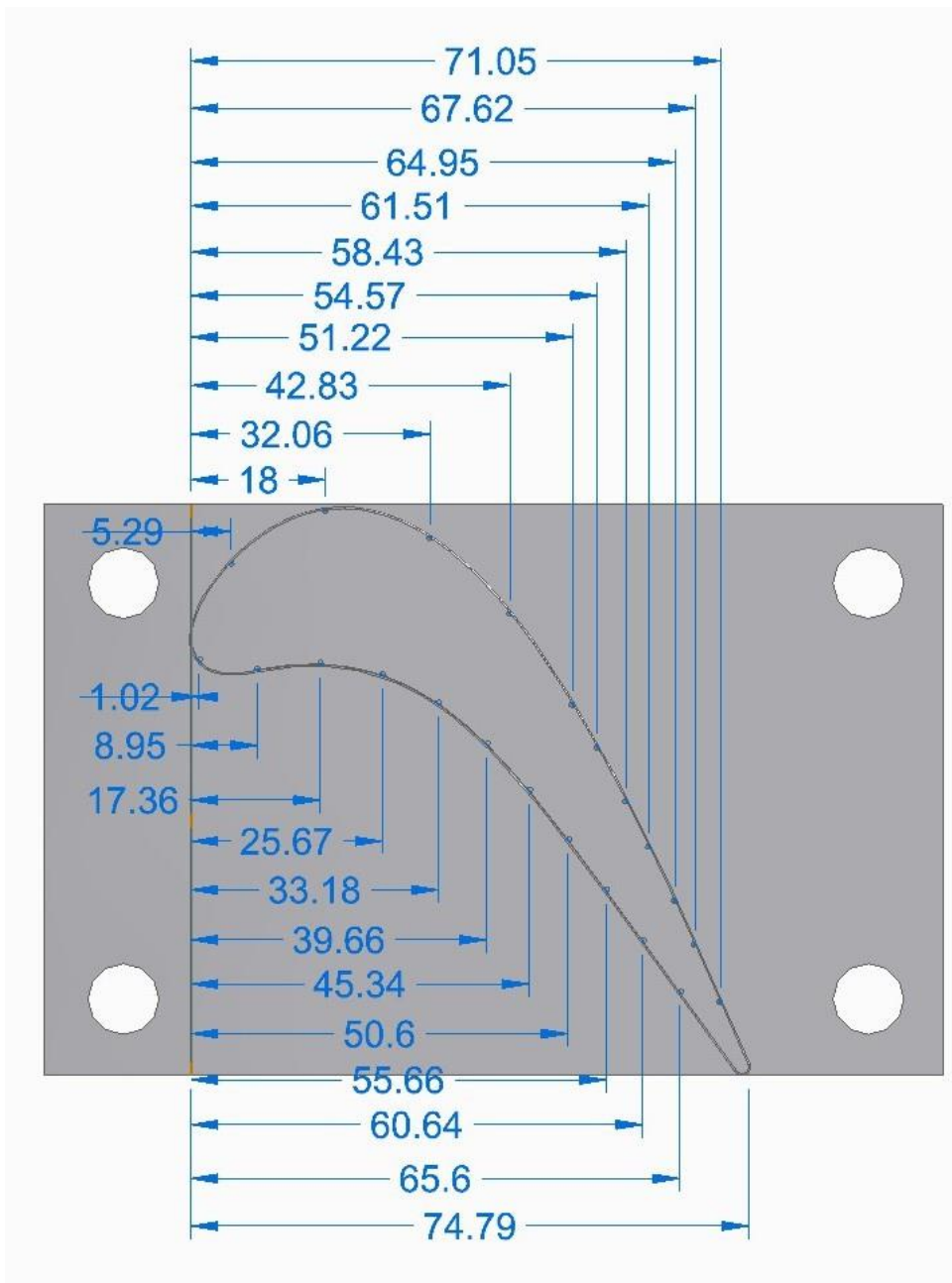


Figure 15. Central turbine blade pressure tap dimensional x locations. Dimensions given in millimeters.

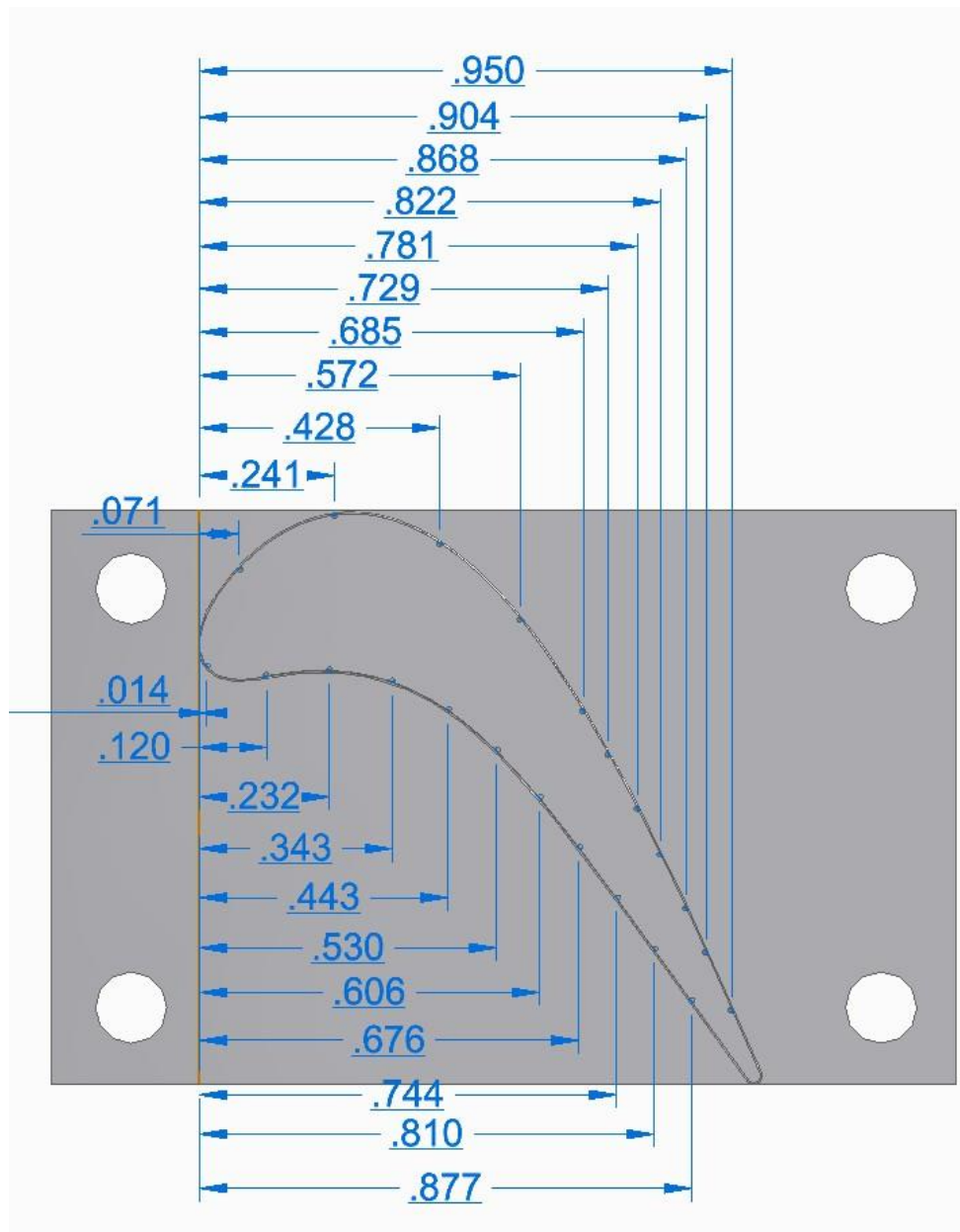


Figure 16. Central turbine blade pressure tap x/C_x locations.

Table 1. Central blade pressure tap locations.

Hole	x (mm)	x/cx	Blade Side
1	1.02	0.013582	PS
2	5.29	0.070628	SS
3	8.95	0.119864	PS
4	17.36	0.232258	PS
5	18.00	0.240747	SS
6	25.67	0.343294	PS
7	32.06	0.428523	SS
8	33.18	0.443463	PS
9	39.66	0.530051	PS
10	42.83	0.572496	SS
11	45.34	0.606112	PS
12	50.60	0.676401	PS
13	51.22	0.68489	SS
14	54.57	0.729372	SS
15	55.66	0.743973	PS
16	58.43	0.781324	SS
17	60.64	0.810526	PS
18	61.51	0.822411	SS
19	64.95	0.868251	SS
20	65.60	0.87708	PS
21	67.62	0.903905	SS
22	71.05	0.949745	SS

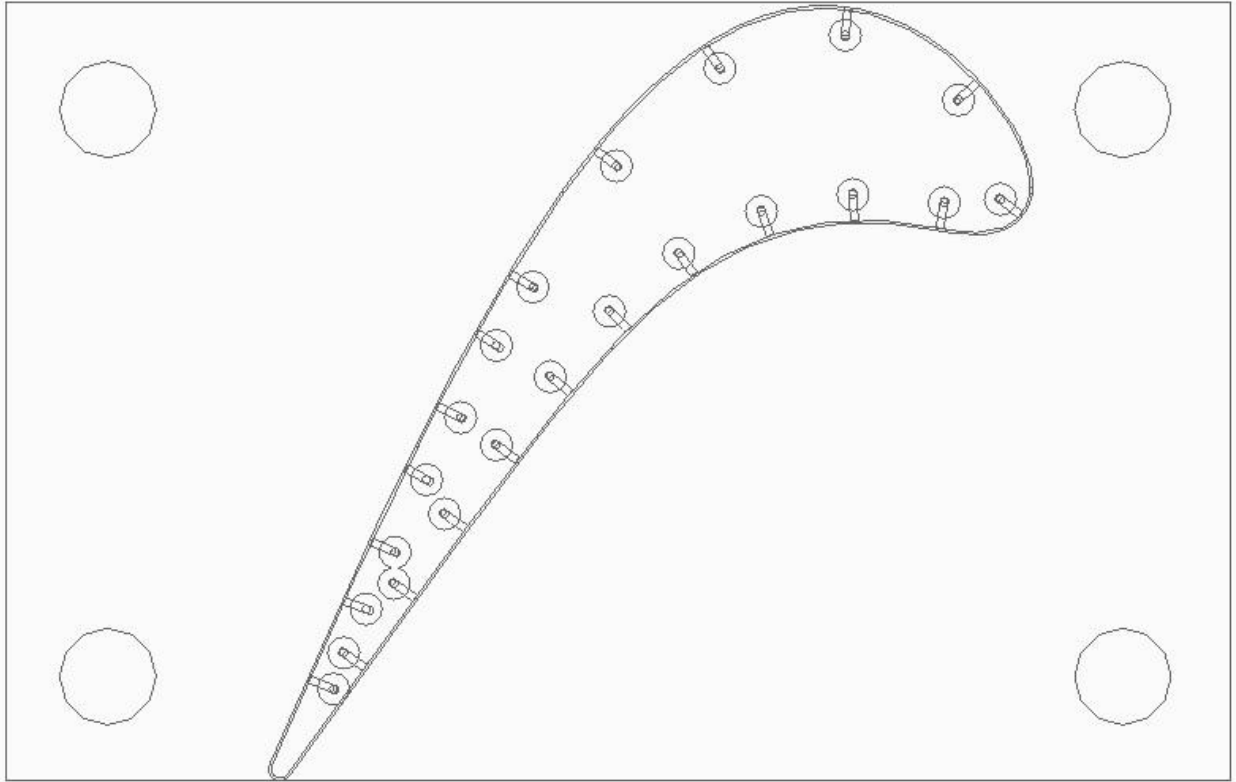


Figure 17. Bottom view of the central turbine blade showing the cooling passage holes with pressure tap connection locations.

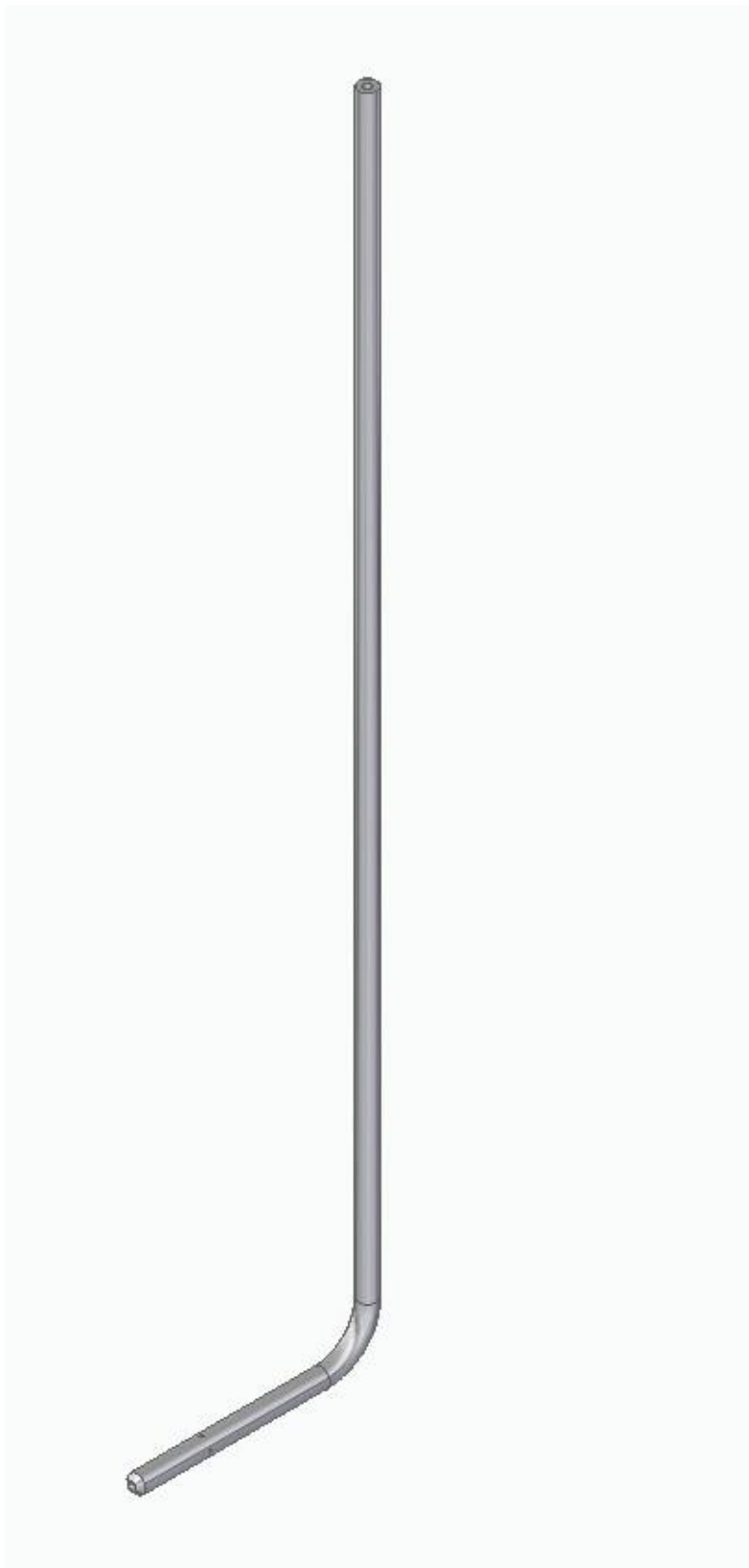


Figure 18. Three-dimensional isometric view of the PCB-6-KL pitot static probe.



Figure 19. Three-dimensional isometric view of the KCC-8 Kiel probe.

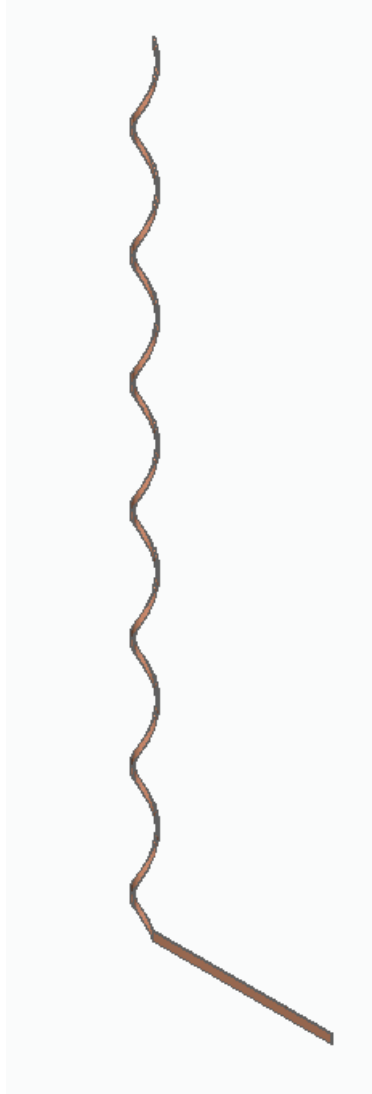


Figure 20. Three-dimensional isometric view of Omega 5TC-GG-T-24-72 Type T thermocouple.

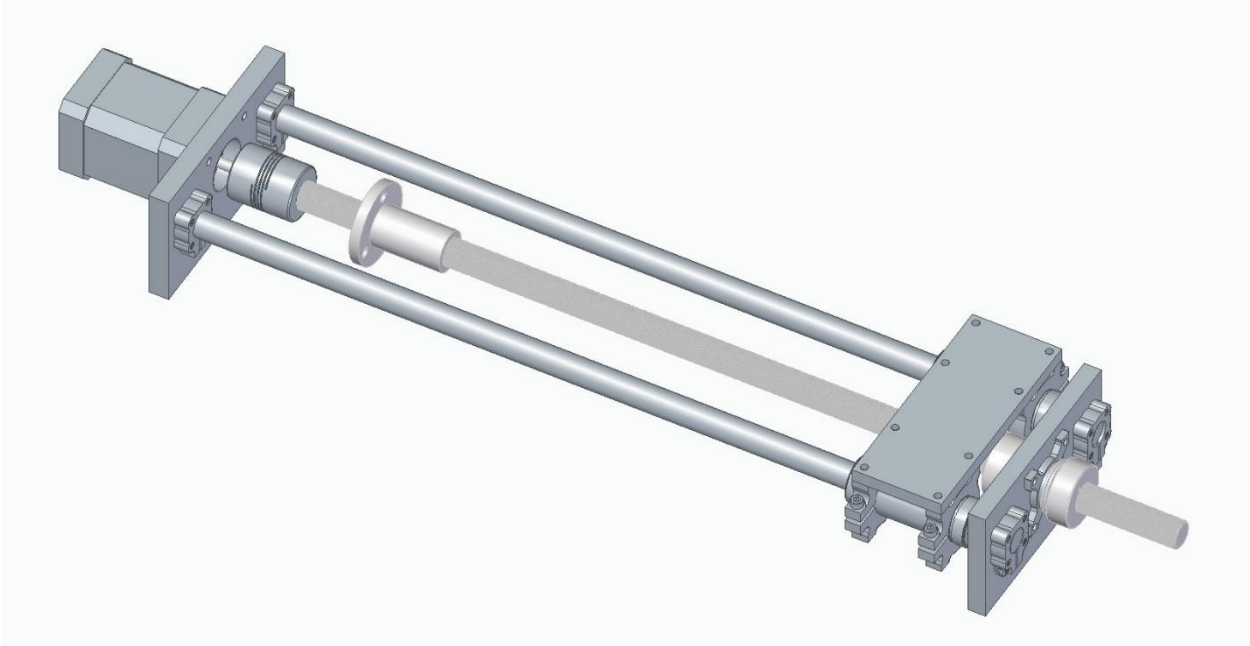


Figure 21. Three-dimensional isometric view of the one-dimensional traverse.

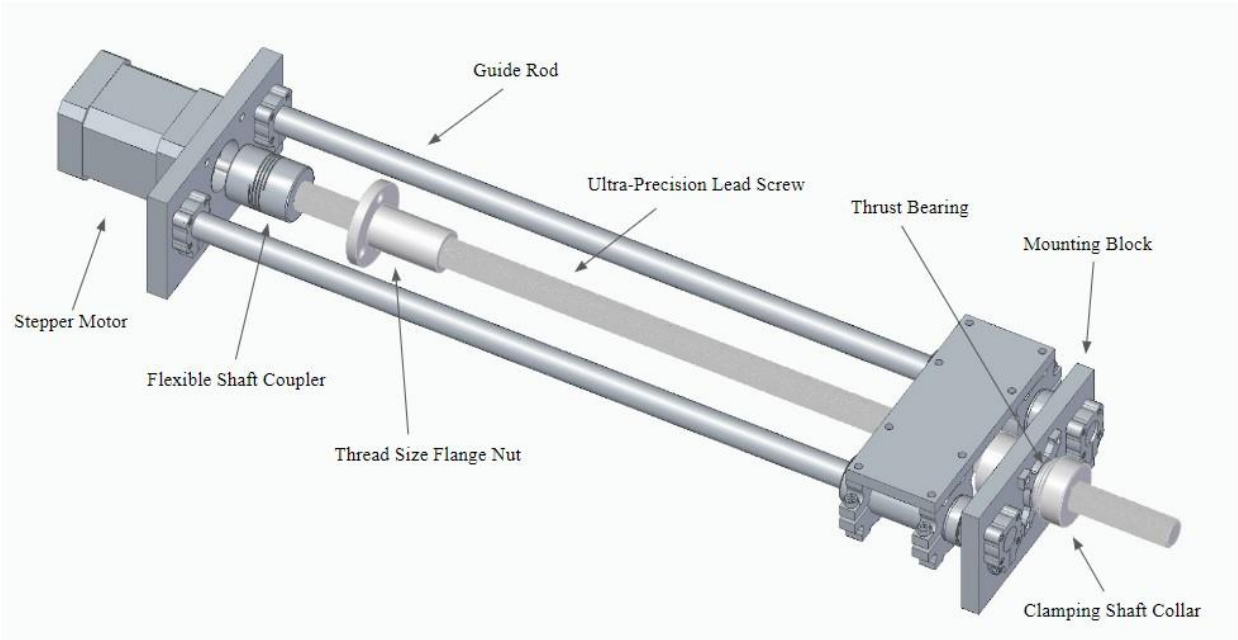


Figure 22. Three-dimensional isometric view of the one-dimensional traverse.

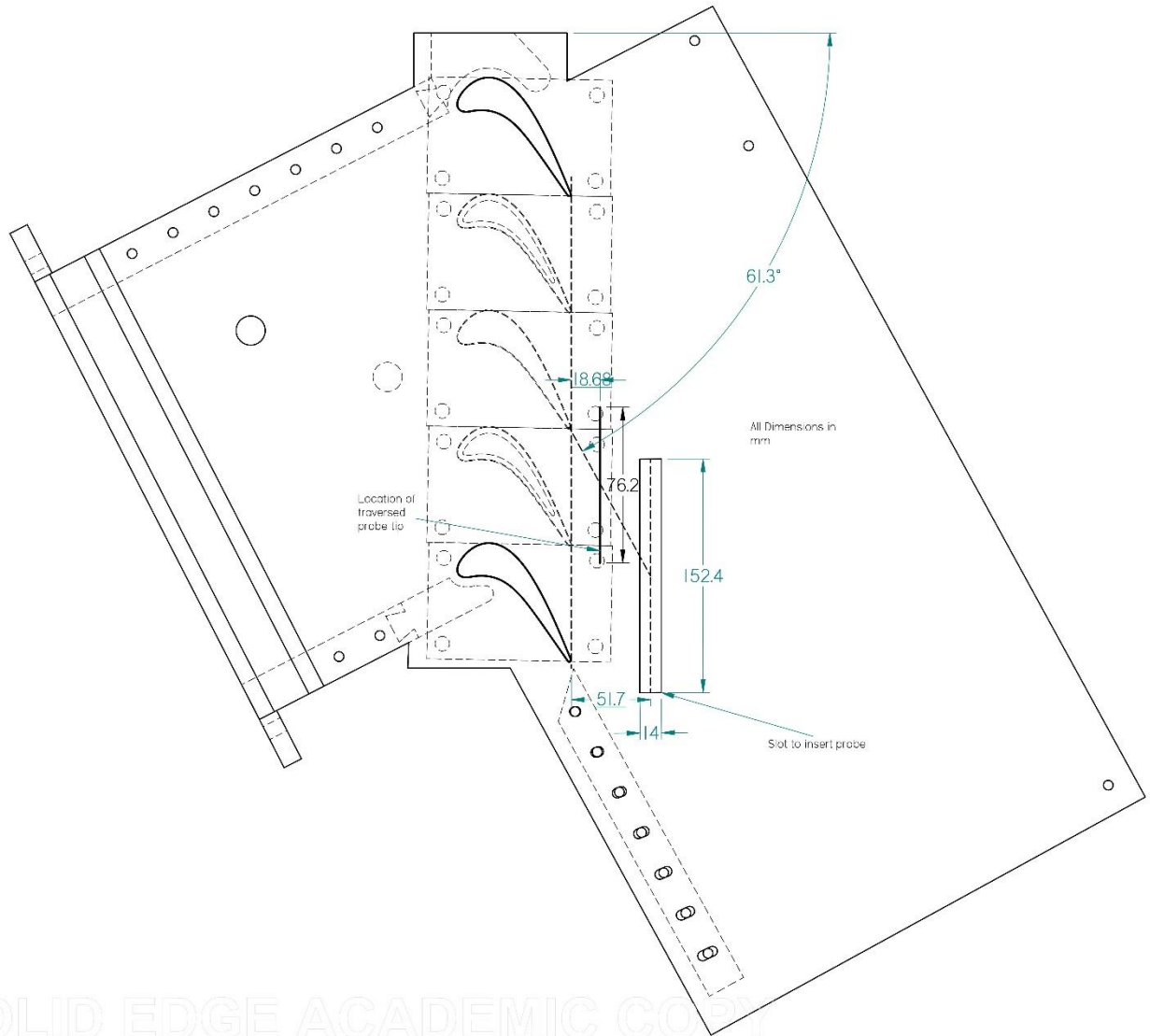


Figure 23. Aerodynamic loss measurement's locations and arrangements.

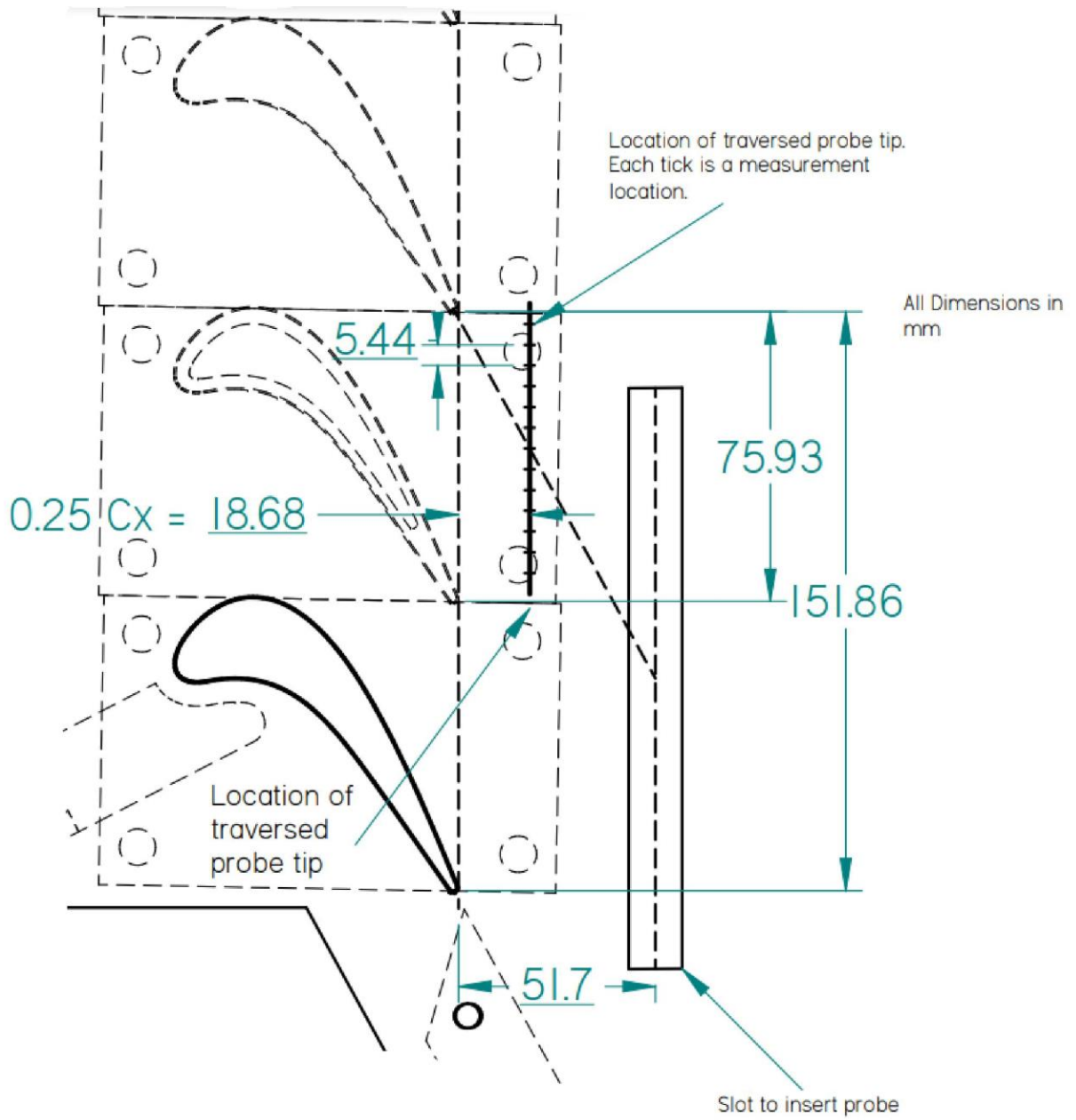


Figure 24. Enlarged view of the aerodynamic loss measurement's locations and arrangements.

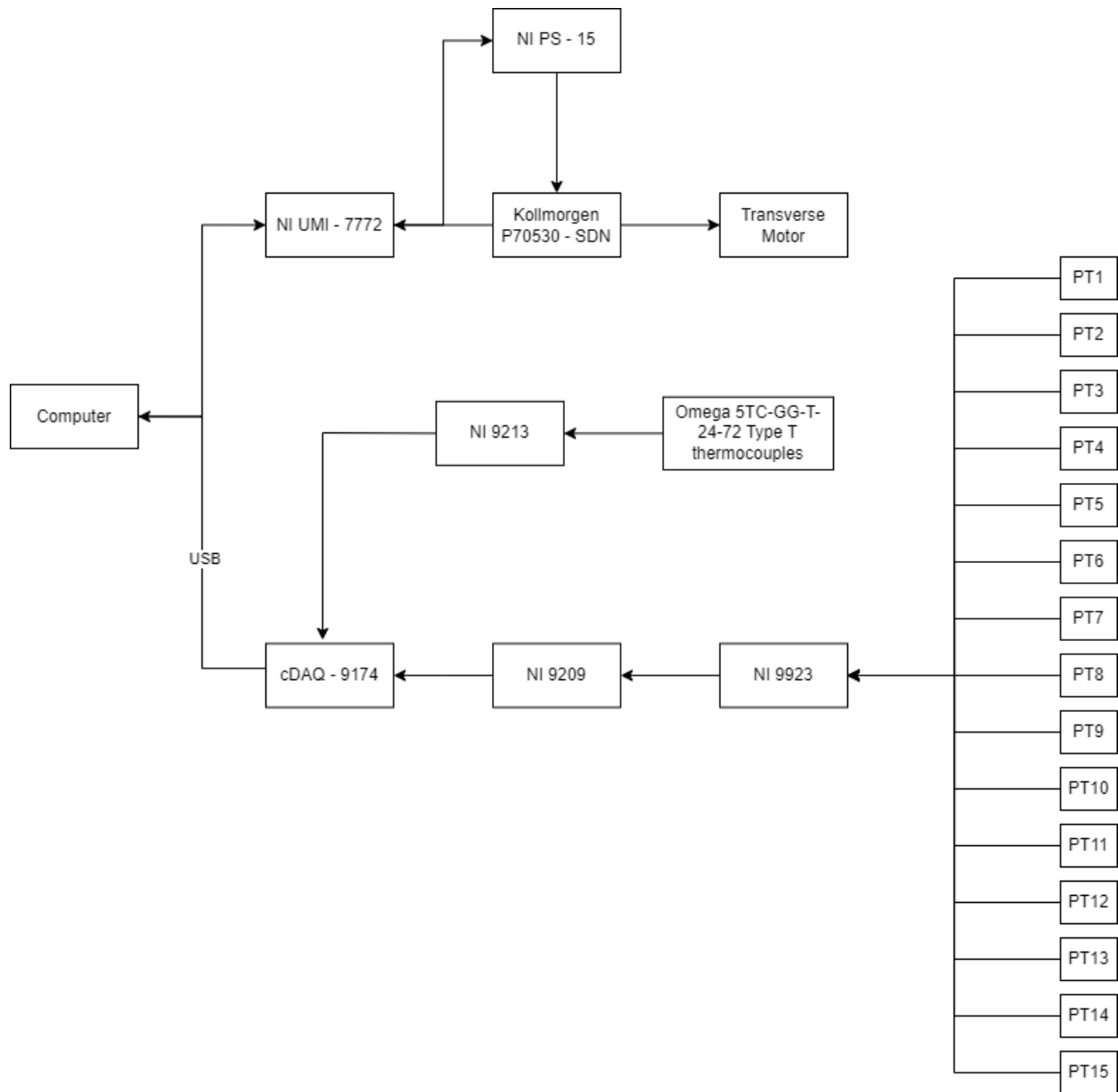


Figure 25. Schematic diagram of the data acquisition system.